Stoch Environ Res Risk Assess (2011) 25:537–554
DOI 10.1007/s00477-010-0420-1

ORIGINAL PAPER

Interannual climate variability in South America: impacts on seasonal precipitation, extreme events, and possible effects of climate change

Alice M. Grimm

Published online: 14 July 2010

Abstract Interannual variability is an important modulator of synoptic and intraseasonal variability in South America. This paper seeks to characterize the main modes of interannual variability of seasonal precipitation and some associated mechanisms. The impact of this variability on the frequency of extreme rainfall events and the possible effect of anthropogenic climate change on this variability are reviewed. The interannual oscillations of the annual total precipitation are mainly due to the variability in austral autumn and summer. While autumn is the dominant rainy season in the northern part of the continent, where the variability is highest (especially in the northeastern part), summer is the rainy season over most of the continent, thanks to a summer monsoon regime. In the monsoon season, the strongest variability occurs near the South Atlantic Convergence Zone (SACZ), which is one of the most important features of the South American monsoon system. In all seasons but summer, the most important source of variability is ENSO (El Niño Southern Oscillation), although ENSO shows a great contribution also in summer. The ENSO impact on the frequency of extreme precipitation events is also important in all seasons, being generally even more significant than the influence on seasonal rainfall totals. Climate change associated with increasing emission of greenhouse gases shows potential to impact seasonal amounts of precipitation in South America, but there is still great uncertainty associated with the projected changes, since there is not much agreement among the models' outputs for most regions in the continent, with the exception of southeastern South America and southern Andes. Climate change can also impact the natural variability modes of seasonal precipitation associated with ENSO.

Keywords Climate variability · Climate change · Precipitation · Extreme events · South America

A. M. Grimm (✉)
Department of Physics, Federal University of Paraná, Curitiba, Brazil
e-mail: grimm@fisica.ufpr.br

1 Introduction

Although the interannual variability makes a smaller contribution than the synoptic and intraseasonal variability to the variance of South America (SA) precipitation, it is very important as a modulator of that higher frequency variability. It has strong impact on monthly and seasonal precipitation totals, and can have impact on the synoptic and even on the intraseasonal variability, and, therefore, on the frequency of extreme events of precipitation.

The interannual climate variability in South America has been studied in specific regions of the continent or in connection with the El Niño Southern Oscillation (ENSO) (e.g. Kousky et al. 1984; Ropelewski and Halpert 1987, 1989; Aceituno 1988; Rao and Hada 1990; Grimm et al. 2000; Grimm 2003, 2004). Only the interannual variability of summer precipitation (December–January–February) has been the object of continental-scale analysis not conditioned to ENSO, using merged precipitation data sets, reconstructed from satellite estimates and gage-based data (Zhou and Lau 2001; Nogués-Paegle and Mo 2002). Recently, motivated by some differences between these two previous continental-scale studies, as well as by the relationships between spring and summer precipitation disclosed by Grimm (2003, 2004) and Grimm et al. (2007), Grimm and Zilli (2009) analyzed the interannual variability of the spring and summer monsoon rainfall in South

America, as well as their connection, with a relatively long series of observed raingage data. The present study carries out analysis that covers all seasons, is continental-wide, and is not restricted to ENSO impacts, although this is the main source of interannual variability.

This paper reviews certain aspects of the climatology and interannual climate variability over SA, while also presenting some new information. The interannual climate variability is emphasized according to its impact on precipitation. The variability modes of precipitation are determined for annual and seasonal precipitation totals, so that the variability can be stressed especially in the rainy season of the different regions of SA (a similar analysis just for Brazil was carried out in Grimm 2009). The influence of climate variability on the frequency of extreme precipitation events is emphasized. Possible impacts of climate change (Keller 2009) on seasonal precipitation are presented and their uncertainties highlighted. Possible impacts on the natural climate variability in SA are also reviewed.

2 Climatic aspects

Figure 1 shows a new and comprehensive perspective of the precipitation regimes over South America. Climatological information is also given in Grimm and Tedeschi (2009), and part of it is reproduced here. The data used for Fig. 1 correspond to the period 1950–2005, and the annual cycles of 2.5° × 2.5° latitude–longitude regions are only represented when more than 25 years of data are available. Low monthly totals in late austral autumn and winter and high values in austral spring and summer indicate a summer monsoon regime over most of the southern hemisphere part of the continent. More information on the climatology, prominent features (such as the South Atlantic Convergence Zone, SACZ, the Bolivian High, and the SA low level jet east of the Andes), and variability of the South American monsoon can be found in the reviews by Nogués-Paegle et al. (2002), Grimm et al. (2005), and Vera et al. (2006).

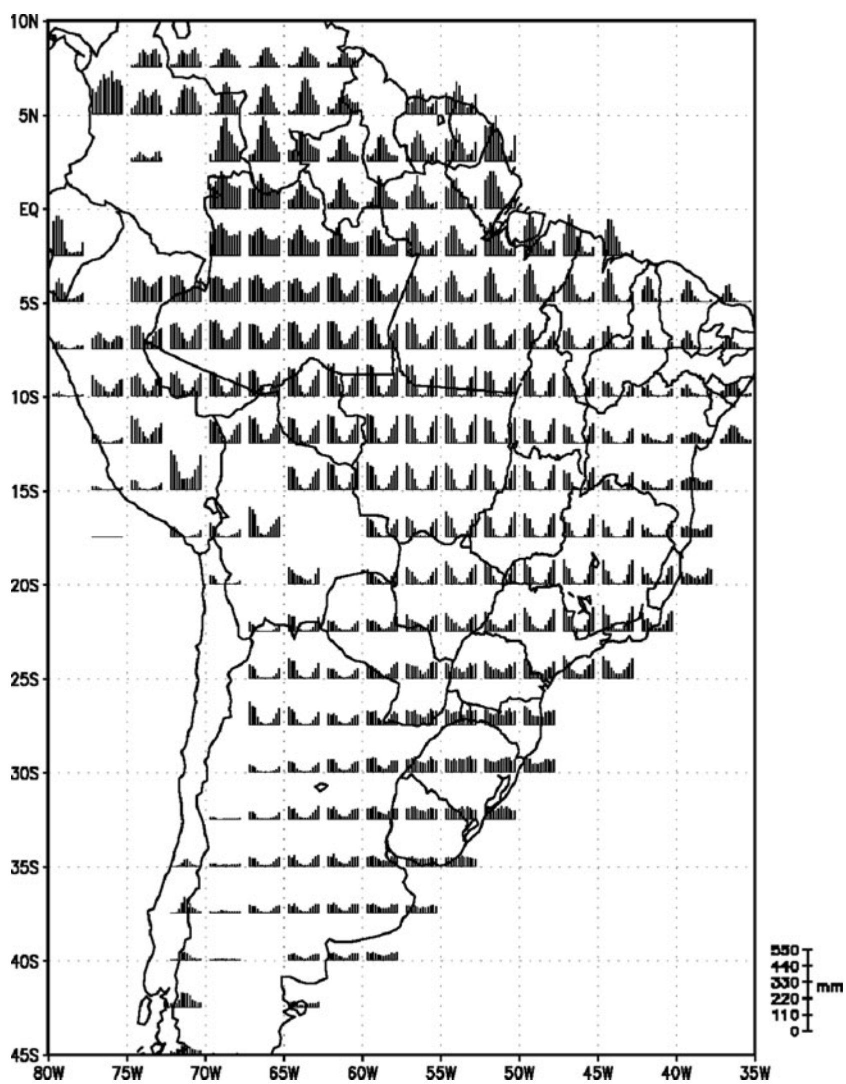

Fig. 1 Annual cycles of precipitation in areas of 2.5° × 2.5° latitude–longitude, calculated with at least 25 years of data for the period 1950–2005

The heaviest precipitation in the wet season starts in the austral spring in Central Brazil (around 10°S, where the wettest season is December–January–February, DJF), and then progresses southward and northward (Nogués-Paegle and Mo 2002, their Fig. 1b; Janowiak and Xie 2003, their Fig. 3), so that in part of southern South America the wettest season is January–February–March (JFM) and nearer the equator it is March–April–May, or even later. Actually, it begins to rain earlier in northwestern Brazil than in Central Brazil, but not above the reference for the onset of the rainy season used in Janowiak and Xie (2003), which is the climatological average of local daily rainfall.

The monsoon starts to demise in March, as the area of deep convection retreats northwestward. Over the north coastal regions of Brazil, deep convection only weakens after late April. In Northeast Brazil, the rainy season takes place during March through May, when the Atlantic intertropical convergence zone (ITCZ) is in its southernmost position. North of the equator, the austral autumn and winter prevail as wet seasons, while the austral summer is relatively dry (Fig. 1). In this region, the peak rainy season is mainly austral autumn in the eastern part, winter in the middle part, and autumn and spring in the western part, in a bimodal regime that reflects the two maxima of solar radiation heating.

South of the equator, winter is the dry season in the tropical belt (0–23°S) of SA, with the exception of parts of the Atlantic coastal region. The monsoon regime with a maximum in summer also prevails in the western part of the subtropical belt (23–35°S), since both the surface heating and the northerly water vapor advection favor the convection during summer in this region. Yet in the eastern part of the subtropics, where water vapor is available throughout the year, the stronger baroclinic conditions of autumn, winter, and spring favor relative maxima in these seasons with respect to summer, although precipitation occurs throughout the year (Fig. 1). Southern Brazil is a region of transition between summer monsoon and mid-latitude winter conditions, which results in peak rainy seasons in January (in the northern part) and July (in the southeastern part), respectively. There is also a region, around the triple border Argentina–Brazil–Paraguay, where the bimodal variation prevails, with wet seasons occurring in March–April and September–October (Grimm et al. 1998). These features may be due to the seasonal change of the upper-tropospheric subtropical jet, and the interaction with the northerly low-level jet east of the Andes (Byerle and Paegle 2002). South of 35°S, in the Andes region of central Chile and immediately to the east of the higher mountains in northern Patagonia, precipitation is conditioned by the seasonal south–north displacement of the South Pacific high, with a maximum in winter and a minimum in summer. East of the Andes, precipitation is very low in mid and high latitudes (Fig. 1).

3 The interannual variability of precipitation

The interannual variability of precipitation over South America is assessed through principal component analysis (PCA) for the period 1961–2000. As the interdecadal variability is not filtered out of the data, it is also present in the modes obtained from the PCA, and appears as a longer period modulation of the interannual variability. The database is from over 10,000 stations, and is submitted to a long and systematic procedure for elimination of spurious data. The main data providers are the Brazilian Agência Nacional de Água (ANA), and hydrometeorological institutes of Argentina, Paraguay, and Uruguay. The gridded datasets compiled by Liebmann and Allured (2005) are also used in order to extend the spatial coverage in northern South America.

The PCA is carried out with annual and seasonal precipitation totals, gridded to 2.5° in order to achieve more homogeneous distribution of data. It allows separation of the main components of the interannual variability of these totals, revealing their spatial distribution and temporal evolution (e.g. Wilks 1995). To emphasize variability in regions with significant precipitation in each season, the PCA is carried out on the covariance matrix of the data, instead of the correlation matrix. The first mode obtained for each season with both procedures is the same, except in winter, when it rains little over most of SA. The possible influence of global sea surface temperature (SST) anomalies on each mode is sought through the correlation of its principal component series with SST series in each $1° \times 1°$ area over the oceans. Since it is not possible to present a detailed analysis of the variability in each season, only the first modes of variability, which explain the largest variance in each season, are shown, with the exception of summer, for which the second mode, associated with ENSO, is also presented.

When referring to the influence of the opposite phases of the El Niño Southern Oscillation (ENSO, El Niño, and La Niña episodes) during specific seasons, we name the year in which an episode begins as year (0) and the following year as year (+). The ENSO impact on SA has been the object of several studies (e.g. Kousky et al. 1984; Ropelewski and Halpert 1987, 1989; Aceituno 1988; Rao and Hada 1990; Pisciottano et al. 1994; Grimm et al. 1998, 2000; Grimm 2003, 2004; Ropelewski and Bell 2008; Grimm and Tedeschi 2009). The anomalous tropical heat sources associated with ENSO events perturb the Walker and Hadley circulation over SA, and generate anomalous Rossby wave trains. In northern SA, the ENSO impact is mainly due to the anomalies of the divergent Walker circulation, as well as to SST anomalies directly associated with ENSO and those produced by ENSO-related atmospheric anomalies in the Atlantic Ocean. In the subtropics and extratropics, the anomalous Rossby waves emanating from the tropics play the most important role, and anomalies in the Hadley circulation may be important. There are also regional processes affecting the ENSO impact in summer.

3.1 Annual precipitation

The first interannual variability mode of annual precipitation over South America is associated with ENSO, as can be seen from the correlation map between its principal component series and sea surface temperature (SST). This map shows the typical ENSO signature in the Pacific SST anomalies (Fig. 2). This indicates that ENSO is the main source of interannual variability in SA. This mode shows negative (positive) anomalies south of 23°S, over southeastern South America (SESA, south Brazil, northeast Argentina, and Uruguay) during La Niña (El Niño) episodes, and positive (negative) rainfall anomalies in northeastern SA, while in the northernmost part of SA the anomalies are opposite (Fig. 2).

The second mode (not shown) features a center of variability over central-east Brazil, near the climatological position of the SACZ, with opposite variations of weaker magnitude in northern and southern SA. It resembles the first mode in summer (see Sect. 3.5). The SACZ is a northwest-southeast band of cloudiness over SA, and is one of the most important features of the South American monsoon system (Grimm et al. 2005, and references therein).

The main contribution to the first mode of annual precipitation seems to come from the variability of the precipitation in the autumn, while the main contribution to the second mode seems to be originated in the summer, as indicated by the resemblance between the first two modes of annual precipitation and the first modes in autumn (see Sect. 3.2) and summer (see Sect. 3.5), and also between their correlation maps with SST.

Besides the correlation with SST, the influence of ENSO episodes on the first annual mode is also manifested by the high factor scores in years with these episodes. For instance, the highest positive peaks of this mode occurred in 1964, 1974, 1985, 1988, and 1989, which were La Niña years, while the strongest negative values occurred in 1983 and 1998, which were El Niño years.

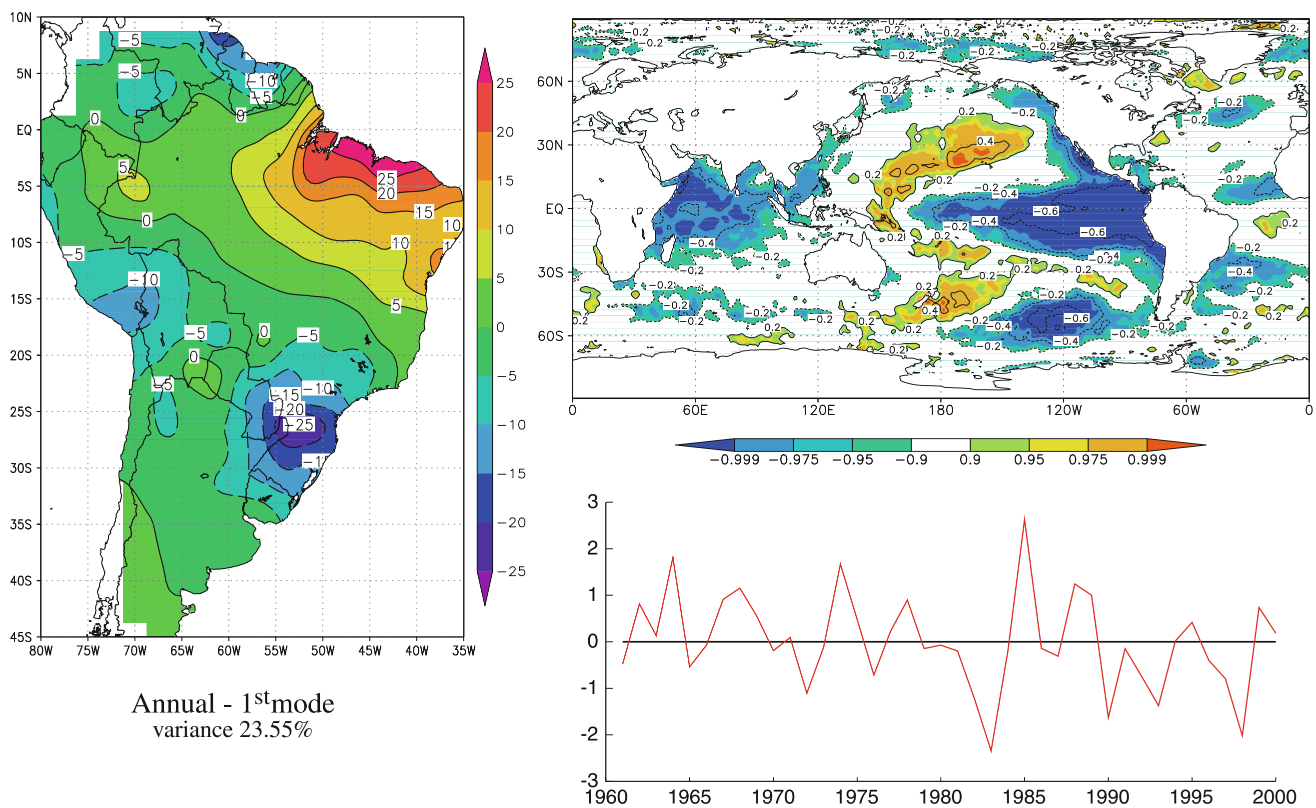

Fig. 2 Spatial distribution (*left panel*) and temporal evolution (*right lower panel*) of the first variability mode of annual total precipitation, with explained variance and the map of correlation coefficients with SST (*right panel*). In this map, the *shades* indicate the levels of confidence (better than 0.90) for positive and negative correlation coefficients

3.2 Autumn

Autumn is the rainy season in northeast Brazil and most of northern SA, and it also rains much in SESA (Fig. 1). The first mode of autumn rainfall variability shows strong components in most of these regions (Fig. 3), in a very similar way as in the first mode of annual precipitation variability (Fig. 2), with strong components over northeastern SA and opposite anomalies in northwestern SA and SESA. The relationship with SST anomalies is similar as well, indicating that this mode is related to ENSO. The most extreme positive and negative factor scores of this mode also occurred in the same years as for the first annual rainfall mode. The ENSO-related SST and convection anomalies in eastern Pacific are mainly responsible for the rainfall anomalies in SESA, through propagation of anomalous atmospheric Rossby waves, while the SST anomalies in the tropical South (North) Atlantic are more connected with the rainfall anomalies in northeastern (northwestern) SA (e.g. Uvo et al. 1998; Giannini et al. 2004). More specifically, it is the anomalous SST gradient between the tropical North Atlantic and the tropical South Atlantic that is important in modulating the Northeast rainfall, through its influence on the position of the ITCZ. Although statistically the association of the autumn rainfall in Northeast is stronger with the meridional SST gradient in the tropical Atlantic than with ENSO (e.g. the Niño3 index), in reality the ENSO influence may be considered as strong. Besides affecting directly the Northeast climate through atmospheric anomalies in the Walker circulation, it also affects the SST gradient in the tropical Atlantic. The ENSO impact on the Northeast rainfall is stronger if the SST anomalies have the same sign in eastern tropical Pacific and in the northern tropical Atlantic, because in this case the direct effect of the ENSO-related atmospheric anomalies is in phase with the effect of the Atlantic SST gradient. This situation is shown in Fig. 3. There is a tendency to opposite anomalies between northeastern SA and the northern part of SA because these two regions undergo opposite influences from anomalous excursions of the Atlantic ITCZ associated with the tropical Atlantic SST meridional gradient (Enfield and Alfaro 1999). This gradient is also related to the Atlantic Multidecadal Oscillation, a SST interdecadal variability mode (Enfield and Mestas-Nuñez 1999) of which there are signs in the correlation map of Fig. 3. This oscillation shows both interannual and interdecadal variability, and is partly responsible for the interdecadal modulation of the first autumn mode shown in Fig. 3.

The ENSO influence on southeastern South America has been responsible for frequent floods in the Paraná/La Plata Basin (e.g. Camilloni and Barros 2000), since there is a

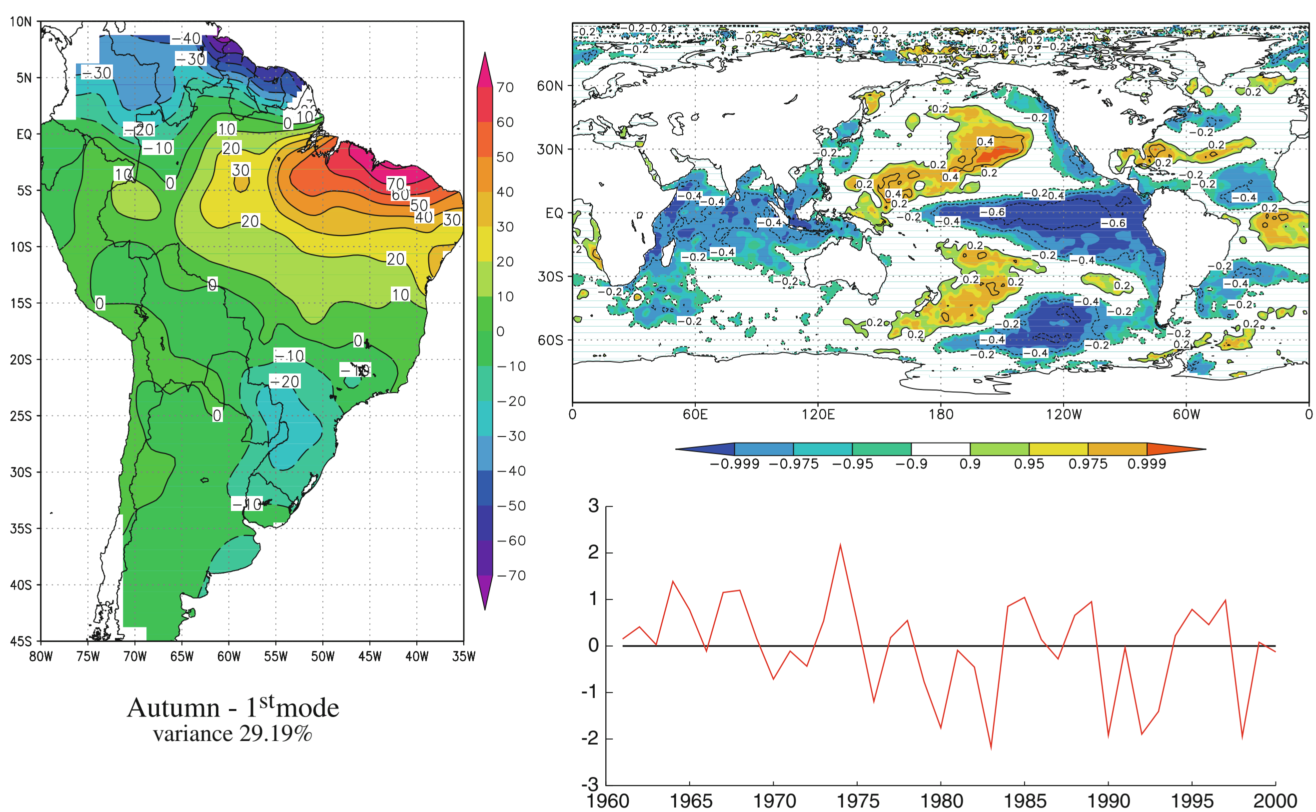

Fig. 3 Same as Fig. 2, for autumn (MAM) precipitation

strong impact of ENSO on the frequency of extreme rainfall events in autumn in this region (Grimm and Tedeschi 2009).

3.3 Winter

Austral winter is the rainy season in parts of northern SA north of the equator, in SESA, and in the extratropical southwestern SA. The first mode shows strong components in the first two of these regions, with opposite signs in the northern and southern parts, and related with ENSO events (Fig. 4). The variability in Chile is not represented in Fig. 4, since data from this region are not available for the whole period of the PCA. Notwithstanding, it is well known that ENSO affects the rainfall in central Chile and neighboring regions in winter (0), increasing it during El Niño and reducing it during La Niña (Aceituno 1988; Rutland and Fuenzalida 1991; Grimm et al. 2000). In SESA, especially in southern Brazil, there is significant ENSO impact in winter (0) and winter (+) (Grimm et al. 1998, 2000). The impact in southern SA is associated with perturbations of the atmospheric circulation over the southwestern Pacific and southeastern Atlantic caused by the ENSO-related anomalous convection in the tropical eastern Pacific. Strong floods associated with extreme precipitation events during winter (+) of El Niño episodes have occurred in southern Brazil (Grimm and Tedeschi 2009).

The ENSO-related perturbations may influence SST anomalies in the southwestern South Atlantic, which appear in Fig. 4, but the SST anomalies in this region may also have other origin independent of ENSO. According to Severov et al. (2004), in the ENSO winter period (April through October), on an average the El Niño events are characterized by negative SST anomalies in the Malvinas current and positive SST anomalies in the Brazil current, and opposite anomalies are observed during the winter of La Niña years. Therefore, the SST gradient off the SESA coast is strengthened (weakened) during El Niño (La Niña) years. This may contribute to enhance the cyclogenesis and consequent rainfall over SESA during El Niño. During winter, as well as in the transition seasons (that is, in the cold semester, from May to September), there is more baroclinicity and, therefore, more baroclinic waves in the westerlies over SESA, which causes more frequent cyclogenesis and frontal penetration. The southern coast of Brazil presents frequent generation of cyclones (Satyamurti et al. 1990; Gan and Rao 1991), and their intensification may receive contribution from the SST gradient near the coast (Sinclair 1995), due to the confluence of the Malvinas

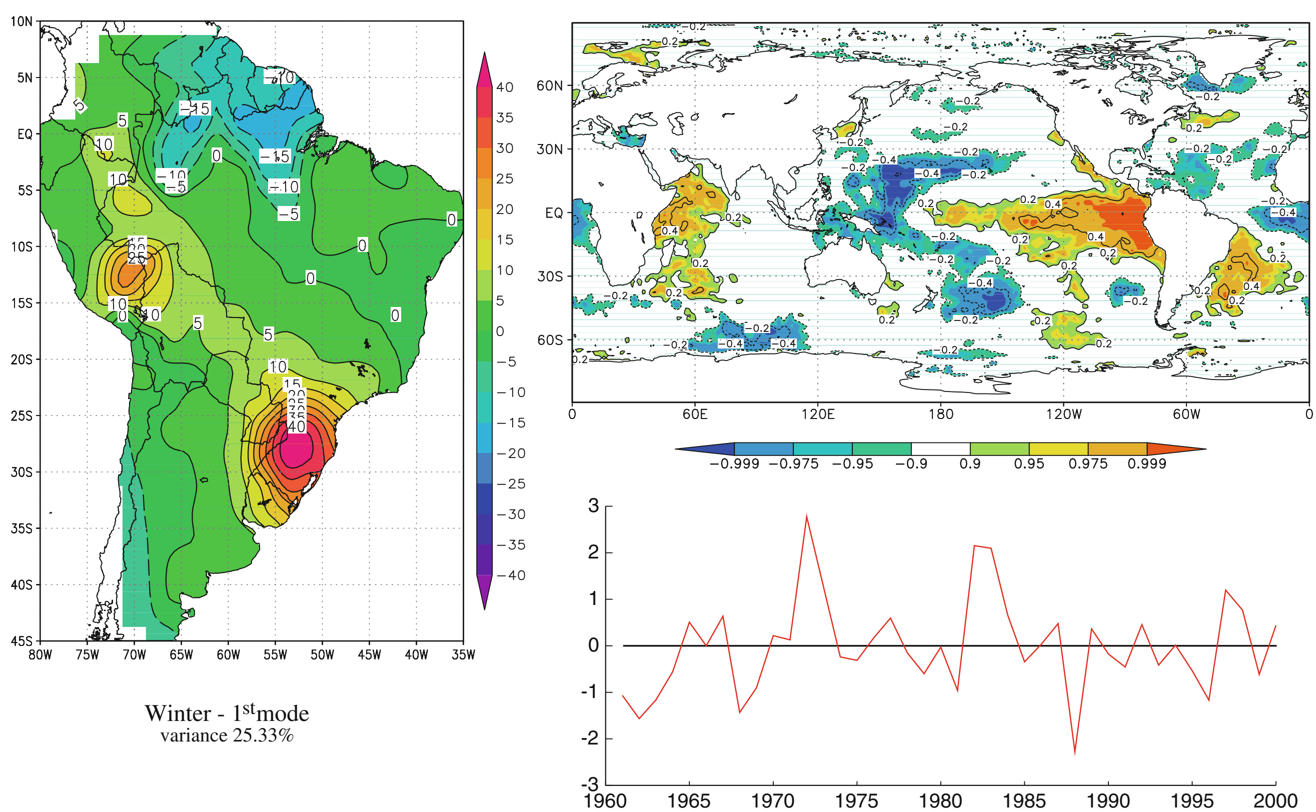

Fig. 4 Same as Fig. 2, for winter (JJA) precipitation

and Brazil currents. The influence of this mechanism is probably reflected in the significant correlations in southwestern South Atlantic, where the warmer SST is associated with higher precipitation in southern Brazil (Fig. 4).

3.4 Spring

Spring is the beginning of the rainy season in most of SA south of the equator, where the monsoon regime prevails. Even in the part of SESA in which the regime is not monsoonal, it rains much in spring (Fig. 1), mainly due to mesoscale convective complexes (MCCs), which are frequent and responsible for a great part of the total precipitation, especially in the transition seasons (e.g. Velasco and Fritsch 1987; Salio et al. 2007; Anabor et al. 2008). Cyclogenesis is also frequent, although it is more intense in winter (Gan and Rao 1991).

The first mode (Fig. 5) exhibits a dipole pattern with regions of inverse variations in Central-East Brazil and SESA (Grimm and Zilli 2009). Since the climatological position of the SACZ is in the southern part of Central-East Brazil, the positive phase of this mode describes weakened convection in the northern edge of the SACZ, while the negative phase indicates a northward extension or shift of the SACZ. This mode presents strong correlation with SST anomalies associated with ENSO, especially the subtropical anomalies in central South Pacific (Barros and Silvestri, 2002). Diaz et al. (1998) found a similar SST pattern when analyzing interannual precipitation variability in Uruguay and the southernmost state of Brazil.

Spring is the season most favorable to teleconnections between SESA and the tropical Pacific Ocean. Therefore, the ENSO impact on the precipitation over SESA is strongest in spring (Grimm et al. 1998, 2000; Grimm 2003, 2004; Cazes-Boezio et al. 2003).

3.5 Summer

Summer is the rainy season over most of SA, due to the predominance of the monsoon regime (e.g. Grimm et al. 2005). The first variability mode (Fig. 6) resembles the first mode in spring, but the components in Central-East Brazil are stronger and more extensive than those in spring, while in SESA they are weaker. This mode is similar to the second variability mode of annual rainfall (not shown). It displays the well known dipole of opposite rainfall anomalies between Central-East Brazil and SESA, although its general structure is that of a tripole, with a third center over northwest SA, mainly north of the equator. It would be tempting to think that this mode represents the persistence of the anomalies in spring, but this is not the case, as was demonstrated by Grimm and Zilli (2009), and is explained

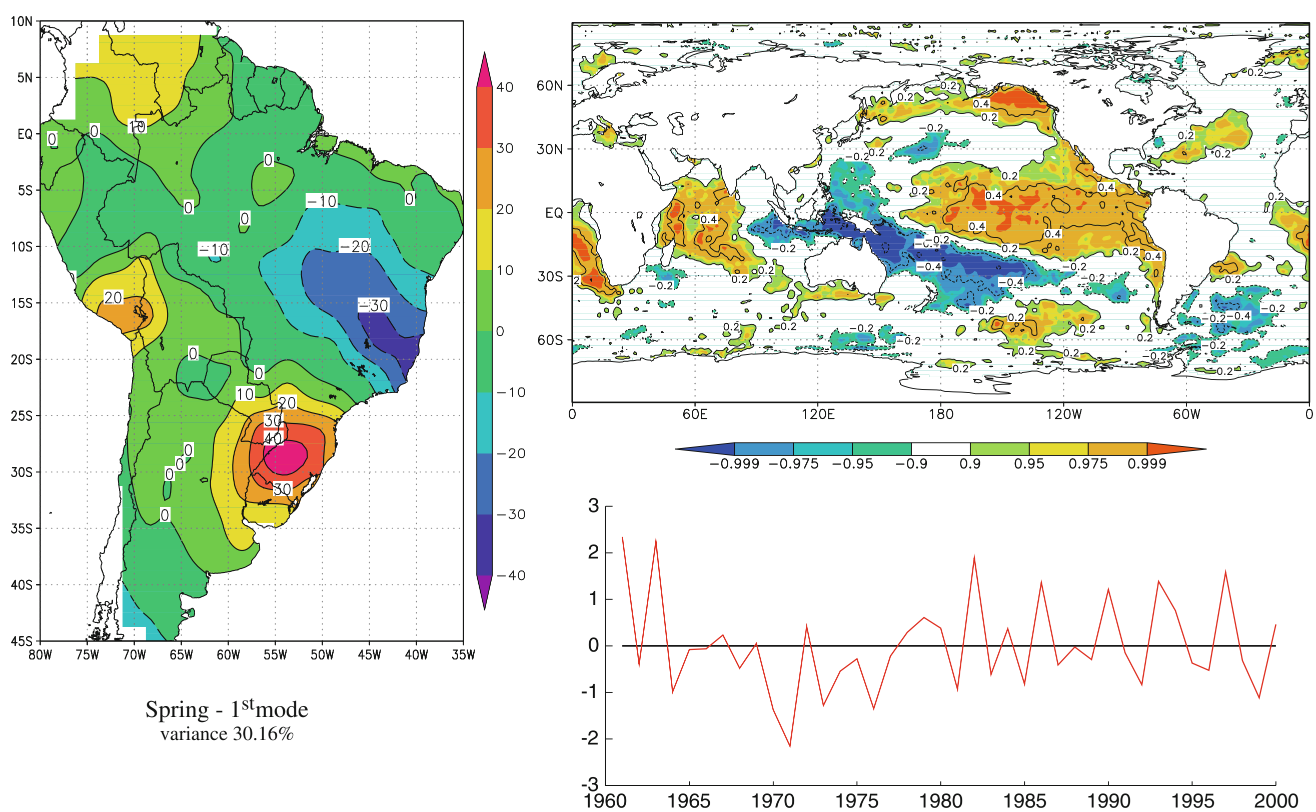

Fig. 5 Same as Fig. 2, for spring (SON) precipitation

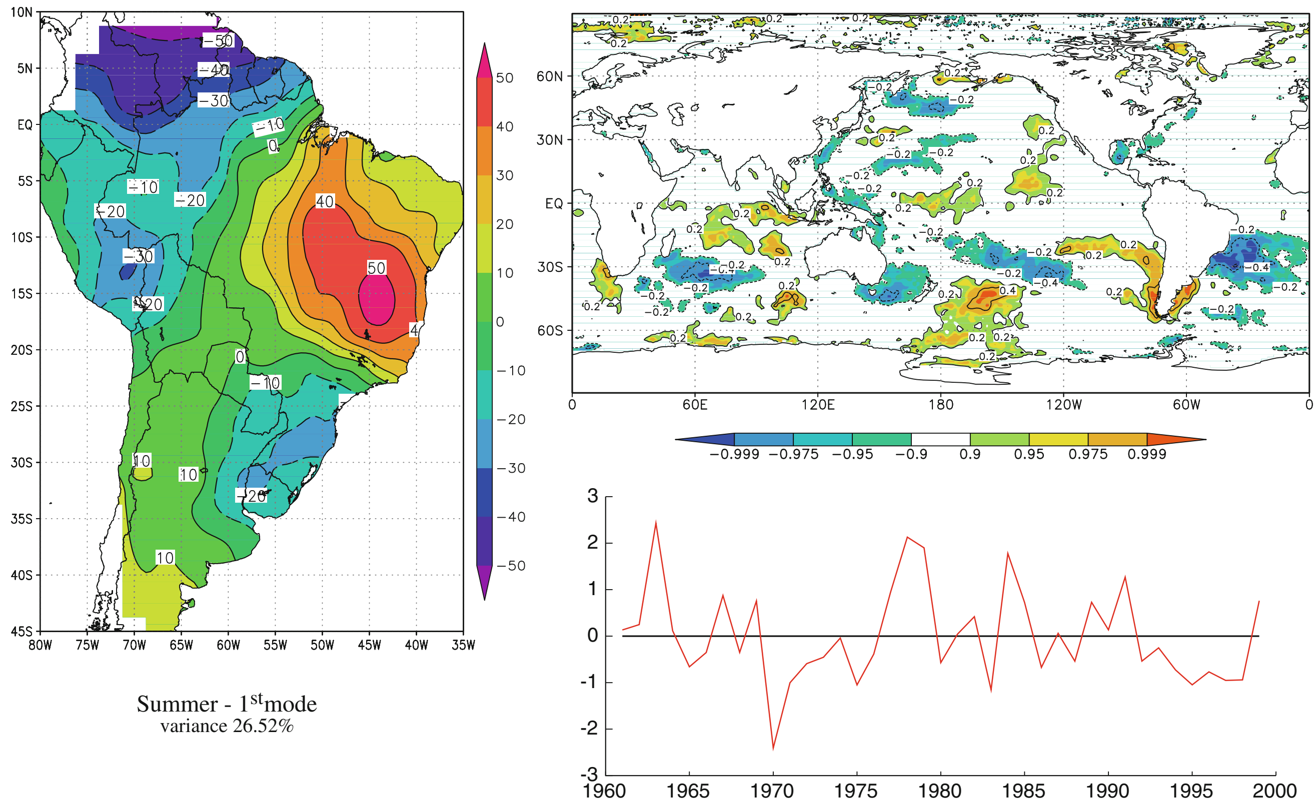

Fig. 6 Same as Fig. 2, for summer (DJF) precipitation

in the following section. The correlation of this mode with SST indicates that there is little remote forcing if compared to spring. The most extensive and strong SST anomaly associated with this mode is located in southwestern South Atlantic, off the southeastern coast of Brazil. This anomaly is due to the influence of the atmosphere on the ocean, and not to a forcing of the atmosphere by the ocean. Greater (less) cloudiness associated with more (less) rainfall over Central-East Brazil (and extending over the ocean) reduces (enhances) the solar radiation flux into the ocean and, therefore, the SST.

In summer, the ENSO-related mode is the second one (Fig. 7), which, contrary to spring, presents same sign of variability in Central-East Brazil and in SESA. It is convenient to emphasize that for similar SST anomalies in the Pacific Ocean the precipitation anomalies in Central-East Brazil are opposite in the ENSO-related modes of spring and summer (Figs. 5 and 7). This is coherent with the results of Grimm (2003, 2004). The anomalies in SESA are weaker and shifted southwestward with respect to spring, which agrees with the findings of Pisciottano et al. (1994), Grimm et al. (1998, 2000), and Diaz et al. (1998). The reversal of the anomalies in Central-East Brazil and the weakening of the anomalies in SESA are coherent with the mechanisms explained in Grimm et al. (2007) and Grimm and Zilli (2009), which are broached in the next section.

3.6 Relationship between the first mode of spring and the first mode of summer precipitation

The first modes of spring and summer, although displaying similar patterns between Central-East Brazil and SESA, have different origins, and do not represent the persistence of similar anomalies from spring to summer. Grimm and Zilli (2009) indicate that there is a significant tendency to reversal of polarity of the dipole between Central-East Brazil and SESA from spring to summer. Previous studies have shown that the precipitation anomalies in spring and summer in Central-East Brazil hold significant inverse relationship, especially in ENSO episodes, when the spring precipitation anomalies are strongest (Grimm 2003, 2004; Grimm et al. 2007). This relationship even affects the relationships between the first modes of interannual variability of precipitation in spring and summer, indicating its importance in a broader context.

These modes are associated with a rotational anomaly over Southeast Brazil (the southern part of what we call Central-East Brazil) that either conveys moisture flux coming from the Atlantic, northwestern SA, and Amazon Basin into Central-East Brazil, decreasing its transport into SESA (if it is cyclonic), or increases the moisture transport into SESA and northwestern SA (if it is anticyclonic). Grimm and Zilli (2009) show the anomalous low-level

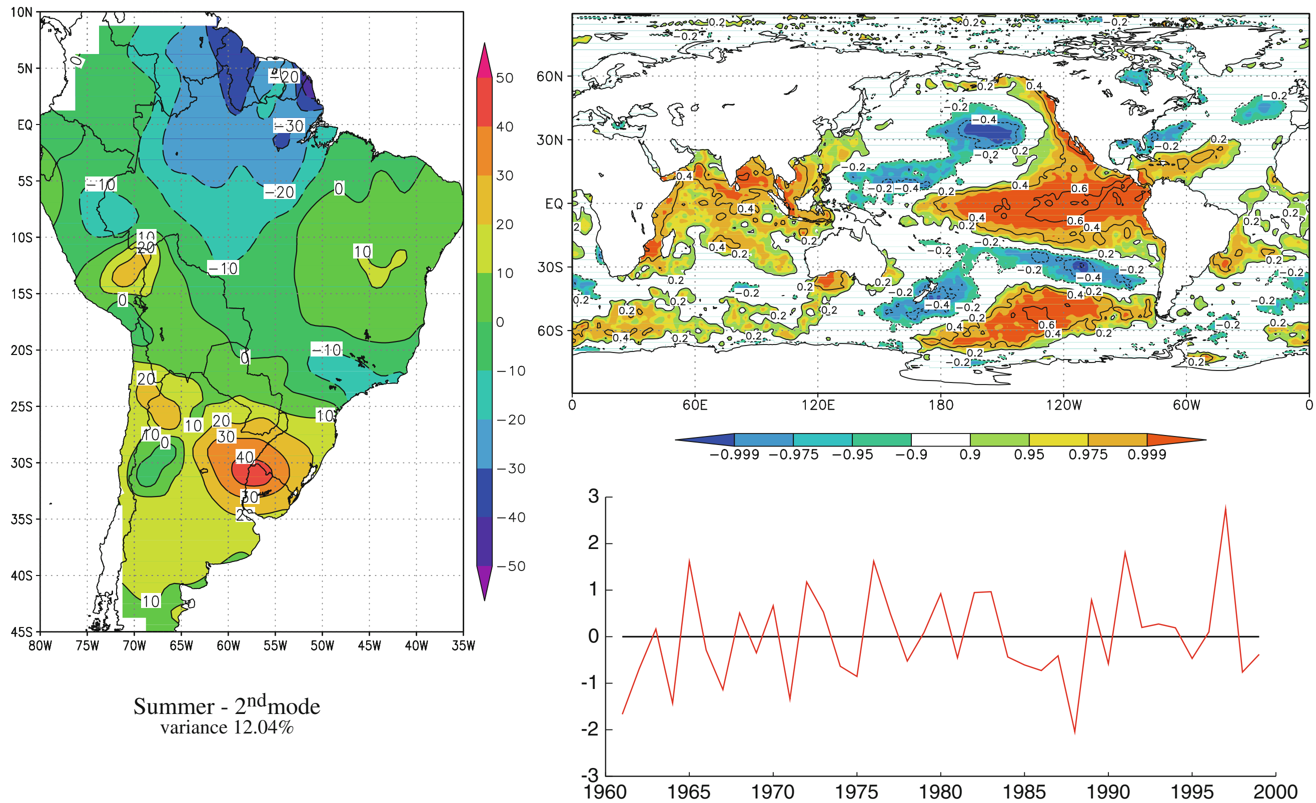

Fig. 7 Same as Fig. 2, for the summer second mode

wind field associated with the first summer mode, giving an idea of the above described moisture flux that is associated with opposite anomalies in SESA and northwestern SA (see their Fig. 8b). In spring, that rotational circulation anomaly seems to be remotely forced (Grimm and Zilli 2009), since there is strong teleconnection between the first spring mode and remote SST (Fig. 5), but after strong rainfall anomalies over Central-East Brazil in spring, it tends to reverse sign in peak summer, inverting the rainfall anomalies. This reversal is hypothesized to be locally forced by surface-atmosphere feedback triggered by the spring anomalies, as weaker teleconnections in summer (e.g. Cazes-Boezio et al. 2003) allow local processes that are stronger in summer to overcome remote forcing (Grimm et al. 2007; Grimm and Zilli 2009).

The hypothesis proposed to explain this inversion suggests that the precipitation anomalies remotely forced in the spring produce soil moisture and near surface temperature anomalies, which alter the surface pressure and wind divergence, which, in conjunction with the mountains in Southeast Brazil, inverts this circulation anomaly and the rainfall anomalies in summer. The SST anomalies off the southeast coast of Brazil in spring (see Fig. 5) also help this effect. Diagnostic and modeling analyses confirm the necessary links for the proposed hypothesis and the importance of the topography in Southeast Brazil in anchoring this circulation over Central-East Brazil (Grimm et al. 2007). These processes are thermally driven, but enhanced by the topographic effect in southeast Brazil.

The significant relationship between peak summer monsoon rainfall and antecedent conditions in spring suggests that the first mode of interannual variability of summer precipitation is not just the result of random sampling of intraseasonal events. This intraseasonal variability, which also shows similar patterns to the first summer mode (e.g. compare Fig. 8b of Grimm and Zilli 2009 with Fig. 6 of Jones and Carvalho 2002) might be favored or hampered, according to its phase, by local circulation anomaly set up by processes triggered by the interannual variability in spring.

4 Climate variability and extreme events

Some important synoptic and mesoscale features responsible for heavy precipitation in SA are significantly affected in intensity and frequency by climate variability, of which the most important example is ENSO. Grimm and Tedeschi (2009) disclosed significant ENSO signals in the frequency and intensity of extreme events over extensive regions of South America during different periods of the El Niño (EN) and La Niña (LN) episodes. Outstanding examples of this modulation are given here for 3 months of the ENSO cycle (Fig. 8, adapted from Grimm and Tedeschi 2009). This study finds evidence that ENSO exerts a more extensive and significant influence on the frequency of extreme rainfall events than on the monthly or seasonal rainfall anomalies. Its impact on the frequency distribution of daily rainfall is relatively stronger in the heavy rainfall tail of the distribution than on moderate and light precipitation. This is an important aspect, since the most dramatic consequences of climate variability are brought about by its influence on extreme events. Although changes in intensity show less significance and spatial coherence than in frequency, they are consistently combined with changes in frequency in several regions, especially in SESA.

At the beginning of the summer monsoon season (in October and November), the number of extreme events decreases in Central-East Brazil (including the SACZ region) in EN episodes and increases in LN episodes (Fig. 8, left). On the other hand, in the same period, the extreme events are increased (reduced) in SESA during EN

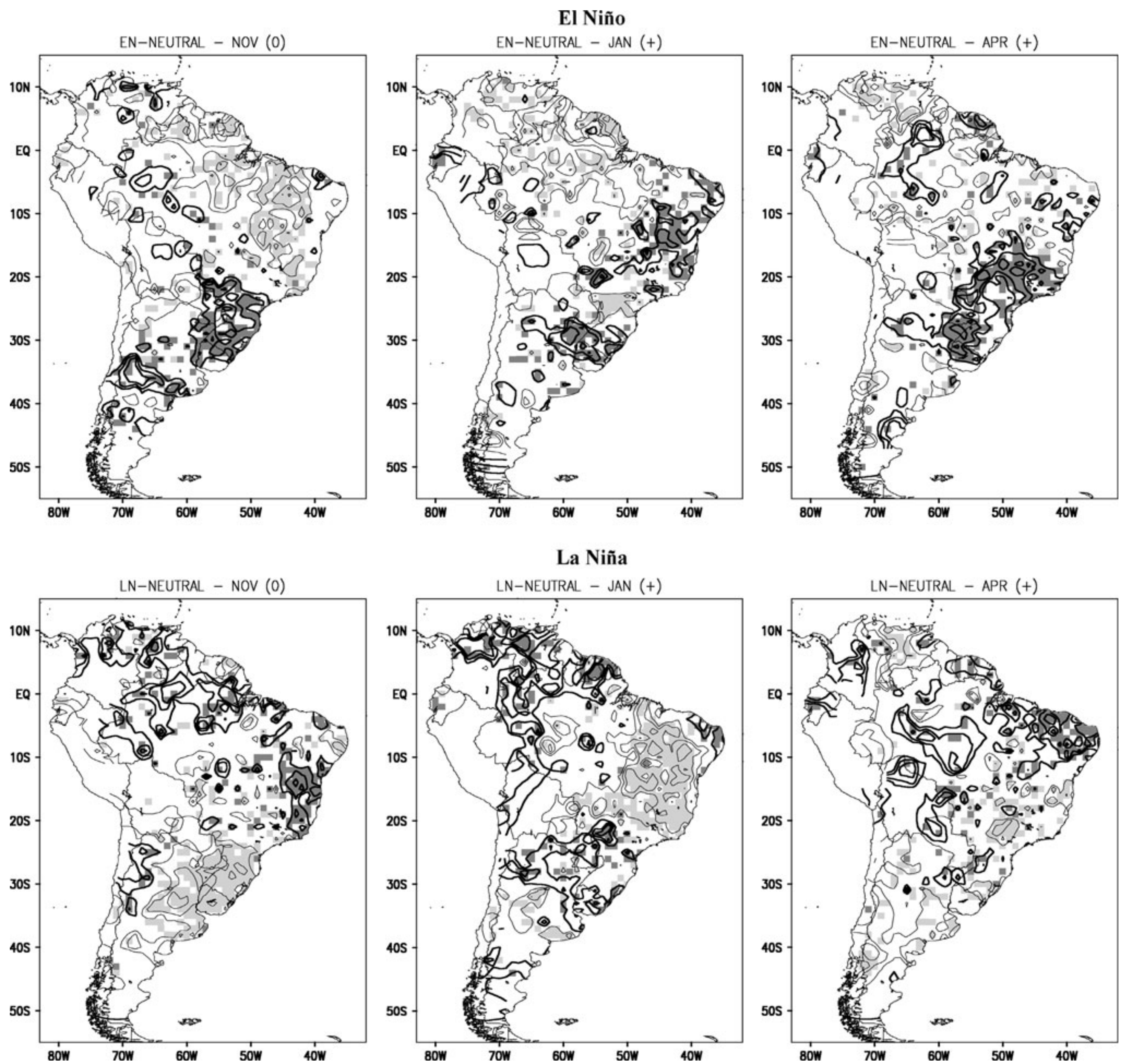

Fig. 8 (*Upper panels*) Differences between numbers of extreme events in El Niño years and neutral years, and (*lower panels*) between numbers of extreme events in La Niña years and neutral years. Contour interval is one event. Positive (negative) differences significant over the 90% confidence level are represented in each grid box by *dark* (*light*) shade. Adapted from Grimm and Tedeschi (2009)

(LN) episodes. Therefore, the mesoscale convective complexes, which are already frequent in SESA in spring, have their frequency and intensity enhanced during EN episodes (Velasco and Fritsch 1987). The reason for this opposite behavior between SESA and Central-East Brazil resides in the anomalous circulation patterns produced by ENSO. During EN, subsidence prevails over Central Brazil, due to perturbed Walker circulation, while a pair of cyclonic/anticyclonic nearly equivalent barotropic anomalies are produced by Rossby wave propagation over western/eastern subtropical South America. At upper levels, these anomalies enhance the subtropical jet and the cyclonic advection over SESA, while at lower levels they produce moisture divergence in Central Brazil and enhance the South American low level jet east of the Andes with its northerly advection of moisture into SESA (Grimm 2003). Opposite anomalies prevail during LN episodes (Grimm 2004).

On the other hand, in peak summer (January) of EN episodes, the number of extreme rainfall events is increased in Central-East Brazil (Fig. 8, center), and extreme precipitation is favored in the SACZ (Carvalho et al. 2004; Grimm and Tedeschi 2009). Yet, in SESA, the number of extreme events is reduced in the northernmost part of the region, but remains enhanced in the southernmost part of Brazil, northern Argentina, and Uruguay. Impacts during LN are approximately opposite (Grimm and Tedeschi 2009). The reversal of ENSO impact on Central-East Brazil from November to January is connected to the inversion of the regional circulation anomaly over Southeast Brazil, which directs moisture either to southern Brazil or to Central-East Brazil (Grimm 2003, 2004), as discussed in the previous section.

In April (+) of EN episodes, the frequency of extreme events is again significantly enhanced in SESA, being connected with some of the strongest floods in the Paraná/La Plata Basin for episodes persisting until the austral autumn (Camilloni and Barros 2000). Corresponding reduction during LN episodes is weaker, less extensive, and the signals are even mixed (Fig. 8, right). During the rainy season in Northeast Brazil (MAM), the most consistent impacts both on extreme events and monthly rainfall occur in March (+) of EN (not shown) and April (+) of LN episodes, pointing to a reduction during EN and an enhancement during LN.

The Amazon River Basin, whose prevalent rainy season is the austral autumn, does not present a uniform ENSO impact on extreme events or even on seasonal precipitation totals, as already shown in Fig. 3, in which the eastern part of the Amazon Basin shows the strongest variability associated with ENSO. However, over the Amazon basin, increased (reduced) occurrence of extreme rainfall events (and monthly totals) prevails during the LN (EN) austral autumn (+), especially during April (+) of LN episodes (Fig. 8, right) (May (+) of EN episodes, not shown). This behavior is even dominant in other seasons, as shown in the other panels of Fig. 8. This produces a tendency to opposite streamflow anomalies of the Amazon River at the end of the rainy season in EN and LN episodes (Marengo and Hastenrath 1993).

5 Climate change perspectives

Before carrying out the assessment of climate change impacts on South America, the performance of several models in reproducing the precipitation climatology in South America is assessed. Then the projected seasonal average precipitation change over the continent from the period 1961–1990 to 2071–2100 is calculated. Finally, a discussion is made on the possible impact of climate change on the first variability modes for spring and summer, based on the analysis by Grimm and Natori (2006).

5.1 Models, data, and methods

We analyze the present-day climate simulations (1961–1990) and climate change scenarios (2071–2100) of three coupled ocean–atmosphere general circulation models (OAGCMs) and two atmospheric general circulation models (AGCMs). The AGCMs are driven by observed SST for the period 1961–1990, and by anomalous SST obtained from the HadCM3 model for the period 2071–2100, added to climatological observed SST. Table 1

Table 1 List of models used to generate simulations analyzed in this study

Center	Model	Reference	Grid
Max Planck Institute für Meteorologie	ECHAM4/OPYC3	Stendel et al. (2000)	~2.813° × 2.813°
Hadley Centre for Climate Prediction and Research	HadCM3	Gordon et al. (2000)	2.5° × 3.75°
Max Planck Institute für Meteorologie	ECHAM5/OM	Roeckner et al. (2003) and Marsland et al. (2003)	1.875° × 1.875°
Hadley Centre for Climate Prediction and Research	HadAM3P	Jones et al. (2005) and Rowell (2005)	1.25° × 1.875°
National Center for Atmospheric Research	CCM3	http://prudence.dmi.dk	1.0° × 1.25°

describes the origin and resolution of these models, and some references for more detailed information. However, as our main conclusions can be illustrated by the results of just two of the models, and as it seems to be physically more consistent to project climate changes with coupled models, we present just the results from two OAGCMs: HadCM3 and ECHAM5-OM.

The analyzed climate change scenarios correspond to the emission scenario IPCC-SRES A2 (category high, Nakicenovic et al. 2000). Some simulations for scenario B2 (medium–high) are also analyzed (not shown), and the differences in the projected climate changes are essentially quantitative, but display similar patterns.

Climate change is here defined as the difference between the climatology predicted by the models for the enhanced emission scenario A2 for the period 2071–2100 and the climatology reproduced by them for the observed concentration of gases and aerosols for the period 1961–1990. The latter period is also used for the validation of the models' performance, carried out by comparing the models' climatology with that obtained from the University of Delaware dataset (Legates and Willmott 1990).

5.2 Skill of the models in reproducing the observed climatology

The models are able to reproduce important features of the precipitation annual cycle over SA, such as the migration of precipitation from northern SA into the subtropics during the spring and early summer and subsequent withdrawal during late summer and early autumn, so that winter is the dry season over most of the continent (compare the observed precipitation climatology in the upper panels of Fig. 9 with the simulated climatology in

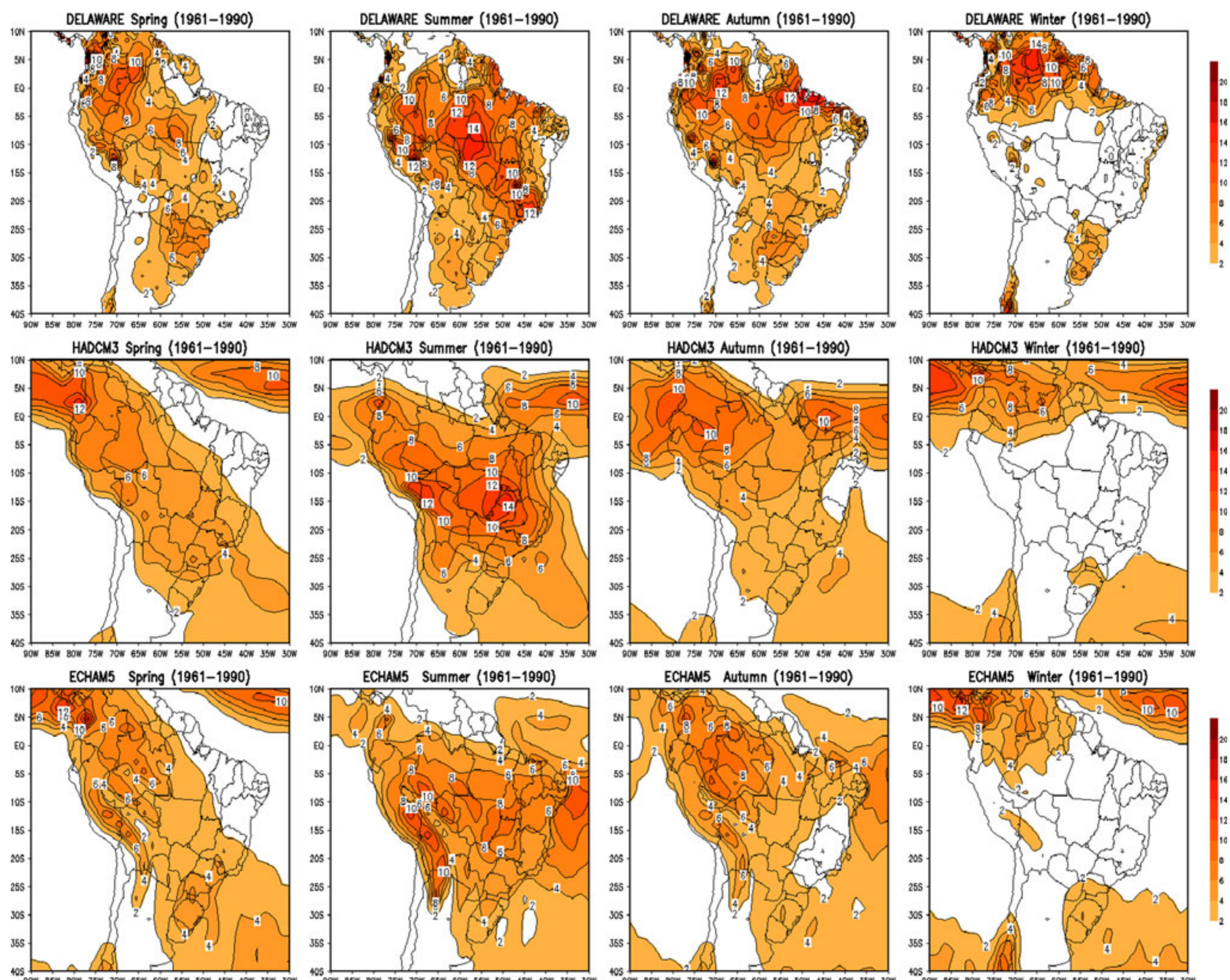

Fig. 9 (*Upper panels*) Observed precipitation climatology (1961–1990) for spring, summer, autumn, and winter from the University of Delaware dataset. (*Middle panels*) Precipitation climatology (1961–1990) reproduced by HadCM3. (*Lower panels*) Precipitation climatology (1961–1990) reproduced by ECHAM5-OM

the middle and lower panels). There are, however, significant inter-model differences in their ability to reproduce the observed precipitation climatology in its more specific aspects. This ability is even season-dependent, for different models present the best performance in different seasons.

The spring main precipitation features and magnitudes are best reproduced by ECHAM5-OM, since the other models (only the HadCM3 is shown) tend to connect the separate centers of maximum precipitation in northwestern SA and SESA.

In summer, the northwest/southeast band of maximum precipitation across SA associated with the SACZ is generically reproduced by the models, although frequently shifted, and with the magnitude of precipitation greatly underestimated, especially in the higher-resolution models. The precipitation maximum in central SA is reproduced in different positions and with very different magnitudes. The magnitude of the SACZ precipitation near the southeast coast of Brazil is underestimated by all models and frequently shifted southward, which might be ascribed to the inability to reproduce the effect of the mountains in this region. Among the two models whose results are shown here, the main features and magnitudes of summer precipitation climatology are best reproduced by HadCM3, but the best simulation among the five models analyzed in this study is from ECHAM4/OPYC3 (not shown).

The northwestward withdrawal of the continental precipitation from summer to autumn and the precipitation maximum in northwest SA is simulated by all models, but most of them do not reproduce other autumn features, such as the strong precipitation in eastern Amazon, the peak rainy season in Northeast Brazil, and the secondary maximum in subtropical SA. The Atlantic ITCZ is displaced to the north by the lower-resolution coupled models. However, in the ECHAM5-OM, the ITCZ reaches the Northeast Brazil coast and precipitation over this region is enhanced. The dry conditions in Central-East Brazil are also better reproduced in this model than in HadCM3. However, the magnitude of precipitation is underestimated, especially in eastern Amazon. The best autumn simulation is provided by the CCM3 (not shown), among the five models analyzed.

The maximum of precipitation in northwestern SA in winter is reproduced by all models, but is generally underestimated. The secondary maximum in southeastern SA is only reproduced in higher-resolution models. The best winter simulation is given by the CCM3 (not shown).

5.3 Climate change scenarios (2071–2100)

The projections of precipitation changes made by the models in response to increasing greenhouse gases and aerosols show great diversity in the tropical region, especially in summer and autumn. This is illustrated in Fig. 10 for HadCM3 and ECHAM5-OM, but is also true for the other models analyzed. Even models that share common dynamical features but have different resolutions (such as

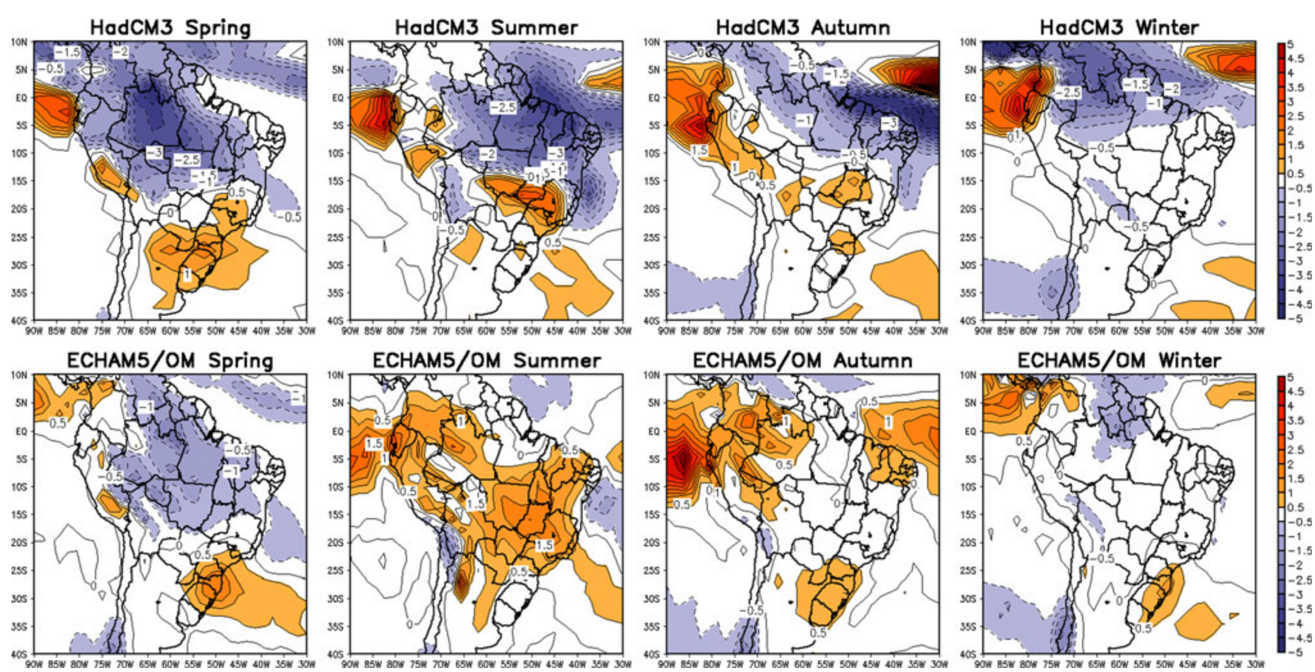

Fig. 10 Changes in precipitation projected by HadCM3 and ECHAM5-OM for 2071–2100

ECHAM4/OPYC3 and ECHAM5/OM) produce different projections (not shown). On the other hand, there are no outstanding discrepancies regarding SESA and the southern Andes. While most of the models project a weak increase of precipitation in SESA, they point to reduction in southern Andes.

There is more convergence in spring and winter. Most of the models indicate decrease of precipitation in most of the Amazon region, with the exception of its western part. Also in these seasons, there are consistent indications of increased precipitation in southeastern SA and reduction in southern Andes.

5.4 Possible impact of climate change on natural climate variability

Grimm and Natori (2006) analyzed the interannual variability of the summer monsoon rainy season in South America and its relationship with SST as simulated by the ocean–atmosphere coupled model ECHAM5-OM for present-day conditions (1961–1990) and future A2 emission scenario (2071–2100). The first mode of the model's precipitation variability, both in spring and summer, is associated with ENSO. These modes (Figs. 11 and 12) correspond, although with significant differences, to the first variability mode of observed spring precipitation (Fig. 5), and to the second variability mode of observed summer precipitation (Fig. 7), which are also associated with ENSO. The main differences reside in the northern half of SA and in the associated SSTs in the Atlantic Ocean. The model overestimates the influence of ENSO in summer.

A comparison of the modes generated by the model for the A2 scenario (Figs. 13 and 14) with the modes generated for the present climate (Figs. 11 and 12) shows that the relationship between ENSO events and precipitation variability in SESA weakens for the A2 scenario, especially in spring, which is presently the season with the strongest

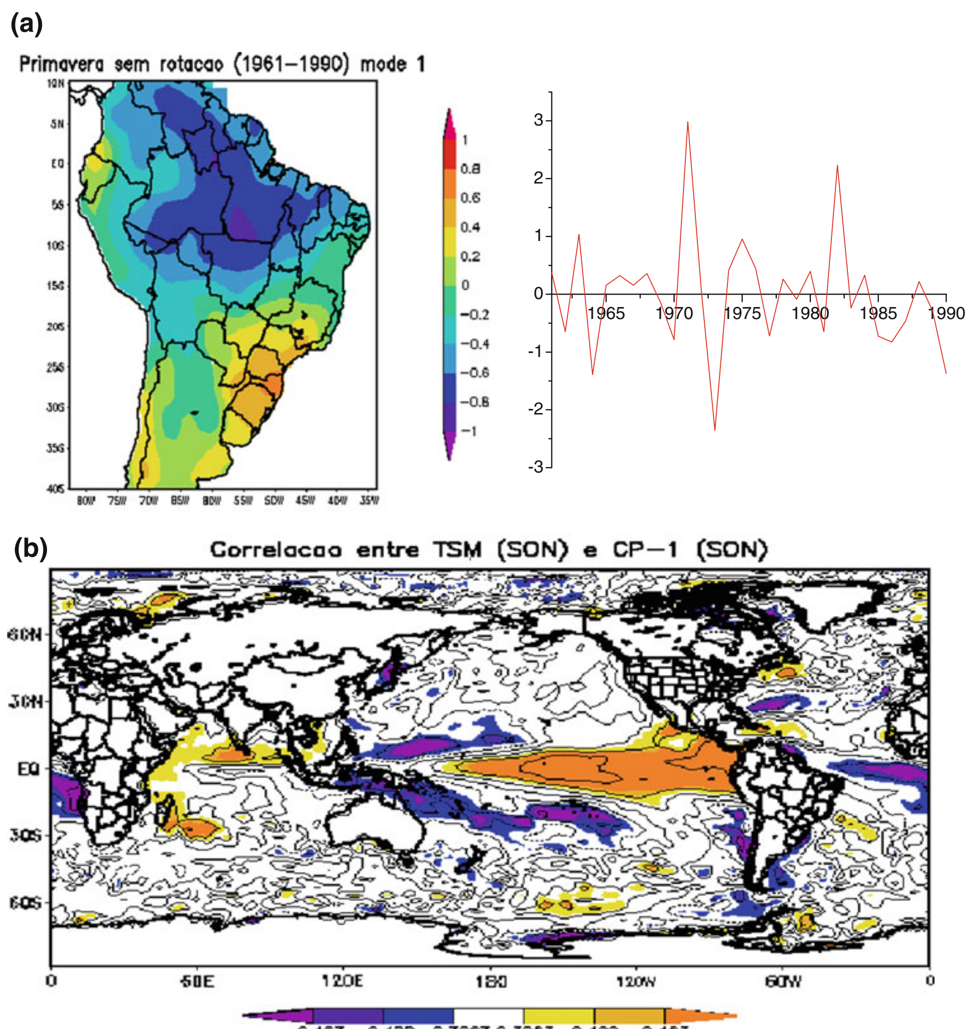

Fig. 11 Factor loadings and factor scores of the first EOF of spring precipitation simulated by ECHAM5-OM for the period 1961–1990 (*top*), and correlation coefficients between factor scores and SST (*bottom*). Correlation coefficients significant to a level better than 0.05 are shaded in *yellow* (positive) and *blue* (negative). This mode explains 20.7% of the variance. Adapted from Grimm and Natori (2006)

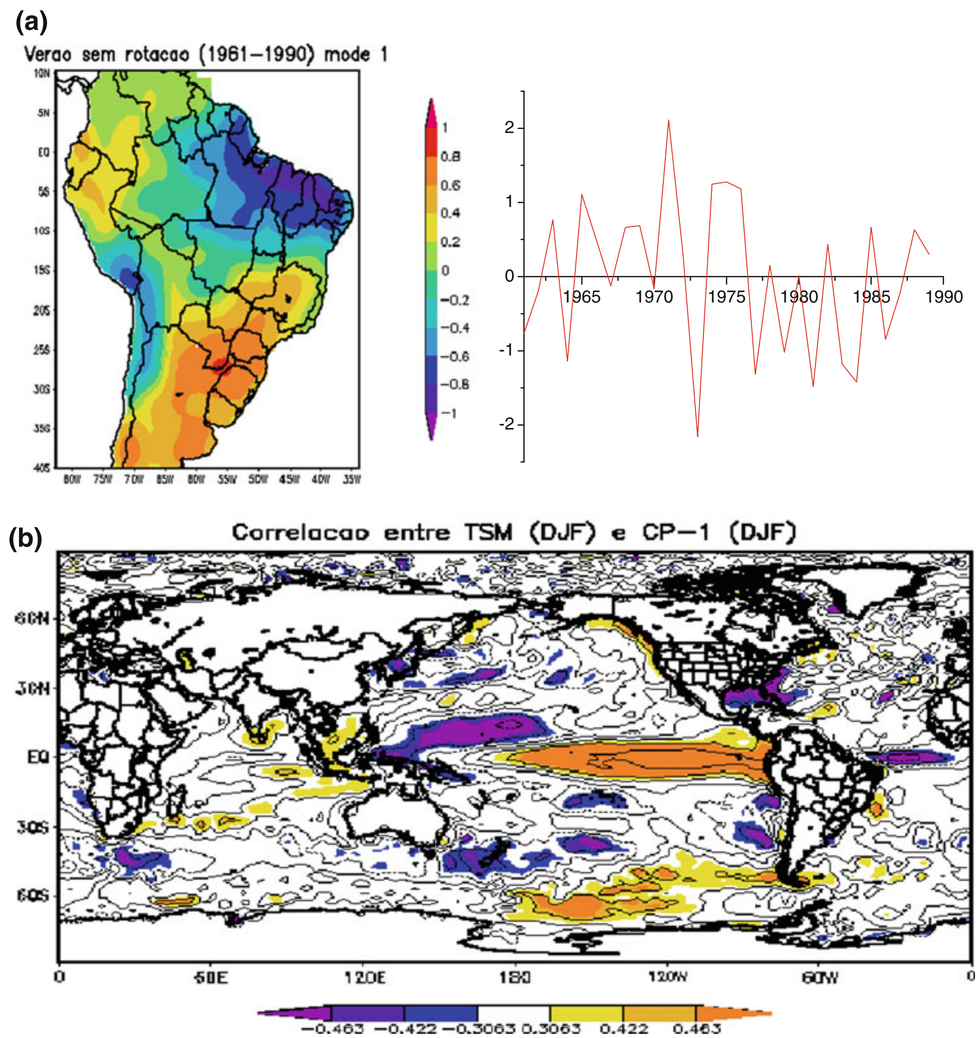

Fig. 12 Factor loadings and factor scores of the first EOF of summer precipitation simulated by ECHAM5-OM in the period 1961–1990 (*top*), and correlation coefficients between factor scores and SST (*bottom*). Correlation coefficients significant to a level better than 0.05 are shaded in *yellow* (positive) and *blue* (negative). This mode explains 22.1% of the variance. Adapted from Grimm and Natori (2006)

ENSO-related impact. On the other hand, it seems to strengthen a little in northern South America, although this projection is less reliable since the ENSO mode is less well reproduced in this region.

The impact of ENSO over southeastern SA precipitation is exerted mainly through anomalous Rossby wave propagation from eastern Pacific towards southeastern SA (e.g. Grimm 2003, 2004). The weakening of the ENSO relationship with SESA in spring in the A2 scenario is visible in the correlation map between SST and the first spring mode (compare Figs. 11 and 13). The correlation with the SST anomalies in the tropical eastern Pacific and subtropical central South Pacific, which are important in producing the convection anomalies that trigger the anomalous Rossby waves, is much weaker for 2071–2100 than for 1961–1990. The reason for the changed teleconnection might be the reduced latitudinal SST gradient in the central Pacific Ocean and the intensification of ENSO in the central Pacific, shown in Grimm and Natori (2006), and the changed atmospheric basic state within which the Rossby waves propagate.

The stronger variability components over Amazonia in the climate change scenario might be produced by enhanced anomalies of Walker circulation associated with the broader area showing significant correlation with SST in the tropical central-eastern Pacific (compare Figs. 11 and 13). The westward shift of the Amazonia center of precipitation anomalies might be associated with the strengthening of the ENSO-related SST anomalies over the equatorial central Pacific, and weakening in the eastern Pacific.

The first summer precipitation variability mode under A2 scenario also shows enhancement and westward shift of the northern center and weakening of the southern center with respect to the present-day conditions (Figs. 12 and 14). The changes in the relationship with SST reported for spring are also observed in summer, but with less intensity. The factor scores series shows clearly a negative tendency,

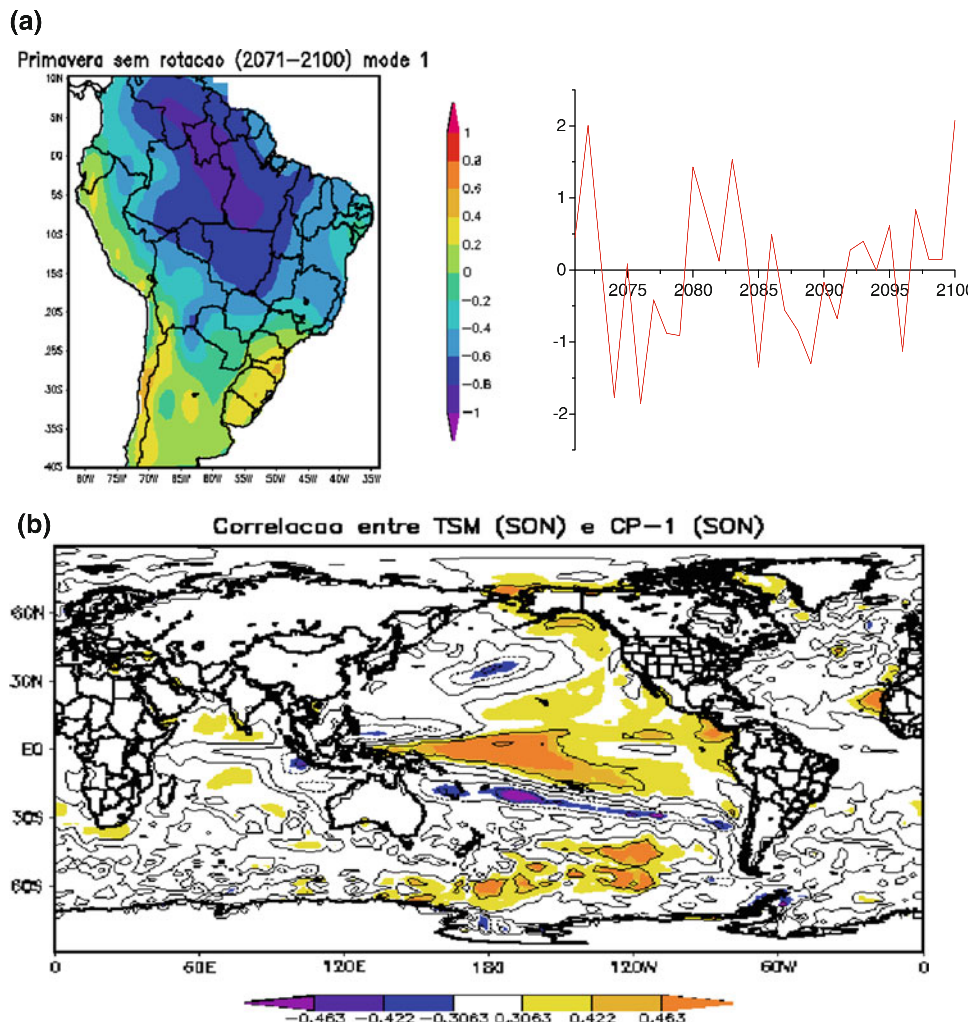

Fig. 13 Factor loadings and factor scores of the first EOF of simulated spring precipitation for the period 2071–2100, assuming the A2 emission scenario (*top*), and correlation coefficients between factor scores and SST (*bottom*). Correlation coefficients significant to a level better than 0.05 are shaded in *yellow* (positive) and *blue* (negative). This mode explains 26.4% of the variance. Adapted from Grimm and Natori (2006)

contrary to spring. This means a tendency to more precipitation in Amazonia in summer, consistent with the climate change for 2071–2100 projected by this model (Fig. 9).

6 Conclusion

Precipitation in South America undergoes strong interannual variability. The most important contribution to annual precipitation variability comes from the variability in autumn. The second more important source of variability is summer, specifically the variations of the SACZ. In all seasons but summer, the most important source of variability is ENSO. In summer, local processes of surface–atmosphere interaction may be more important than remote forcing, since teleconnections into subtropical SA through extratropical propagation of Rossby waves from the tropical Pacific Ocean is not favored in summer (Grimm 2003; Cazes-Boezio et al. 2003; Grimm and Zilli 2009). In summer and spring, the variability is dominated by a dipole-like mode with centers of opposite anomalies in Central-East Brazil and SESA, although in summer this mode also shows strong components in northwestern SA. While in spring this mode is associated with ENSO-related SST anomalies, in summer the main association is with a SST anomaly pattern off the eastern Brazil coast, indicating a local influence of the atmosphere on the ocean. Since there is a tendency to inverse relationship between these dipolar modes in spring and summer, one might hypothesize that the precedent conditions in spring in Central-East Brazil dictate the evolution of mean anomalies in the summer (Grimm et al. 2007; Grimm and Zilli 2009).

Climate change associated with increasing emission of greenhouse gases has the potential to change seasonal amounts of precipitation in SA, and also the natural variability modes of seasonal precipitation associated with ENSO, as shown by simulations and projections made by

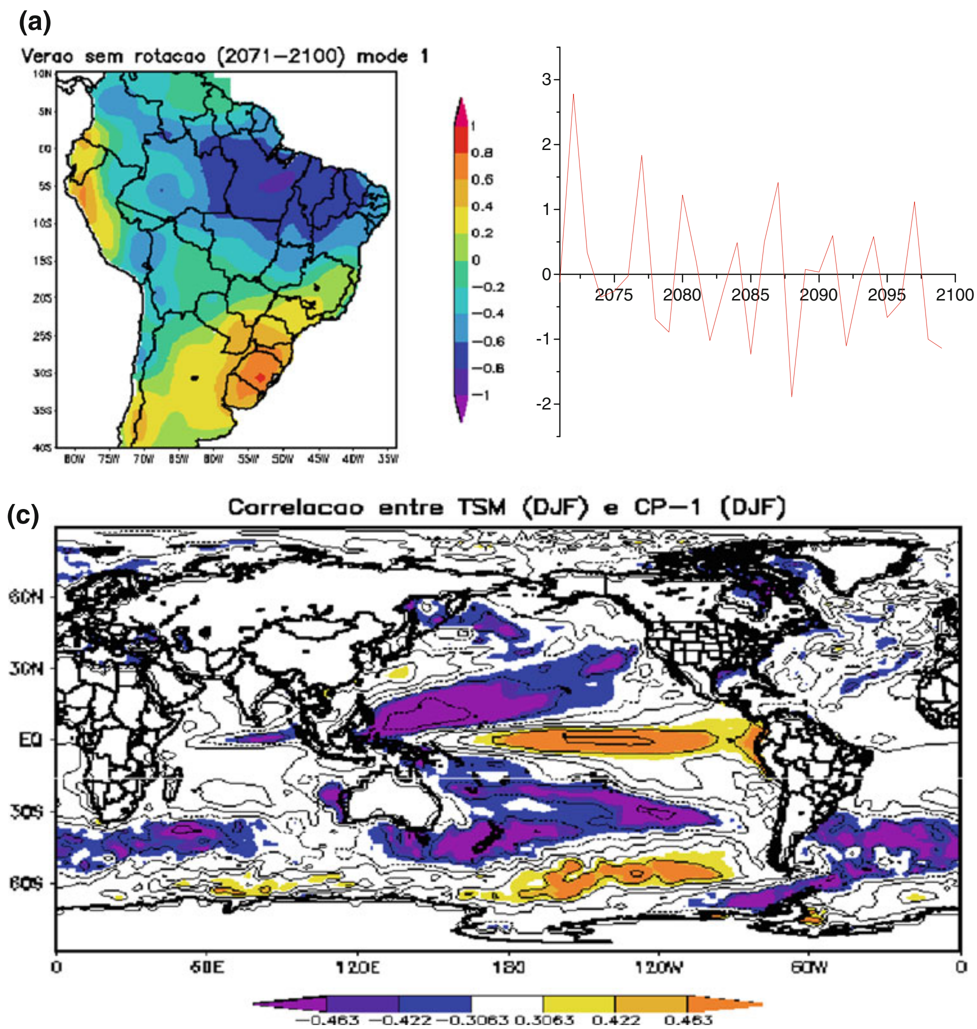

Fig. 14 Factor loadings and factor scores of the first EOF of simulated summer precipitation in the period 2071–2100, assuming the A2 emission scenario (*top*), and correlation coefficients between factor scores and SST (*bottom*). Correlation coefficients significant to a level better than 0.05 are shaded in *yellow* (positive) and *blue* (negative). This mode explains 21.1% of the variance. Adapted from Grimm and Natori (2006)

many models. However, there is still great uncertainty associated with these projections.

Acknowledgments The research leading to these results has received funding from CNPq (Brazilian National Council for Scientific and Technologic Development), and from the European Community's Seventh Framework Programme (FP7/2007-2013) under Grant Agreement no. 212492 (CLARIS LPB. A Europe-South America Network for Climate Change Assessment and Impact Studies in La Plata Basin).

References

Aceituno P (1988) On the functioning of the Southern Oscillation in the South American sector. Part I: surface climate. Mon Wea Rev 116:505–524

Anabor V, Stensrud DJ, Moraes OLL (2008) Serial upstream-propagating mesoscale convective system events over Southeastern South America. Mon Wea Rev 136:3087–3105

Barros VR, Silvestri GE (2002) The relation between sea surface temperature at the subtropical South-Central Pacific and precipitation in Southeastern South America. J Clim 15:251–267

Byerle LA, Paegle J (2002) Description of the seasonal cycle of low-level flows flanking the Andes and their interannual variability. Meteorologica 27:71–88

Camilloni I, Barros VR (2000) The Parana River response to El Niño 1982–1983 and 1997–1998 events. J Hydrometeorol 1:412–430

Carvalho LMV, Jones C, Liebmann B (2004) The South Atlantic convergence zone: intensity, form, persistence, and relationships with intraseasonal to interannual activity and extreme rainfall. J Clim 17:88–108

Cazes-Boezio G, Robertson AW, Mechoso CR (2003) Seasonal dependence of ENSO teleconnections over South America and relationships with precipitation in Uruguay. J Clim 16:1159–1176

Diaz AE, Studzinski CD, Mechoso CR (1998) Relationship between precipitation anomalies in Uruguay and southern Brazil and sea surface temperature in the Pacific and Atlantic oceans. J Clim 11:251–271

Enfield D, Alfaro E (1999) The dependence of Caribbean rainfall on the interaction in the Tropical Atlantic and Pacific Oceans. J Clim 12:2093–2103

Enfield D, Mestas-Nuñez AM (1999) Multiscale variabilities in global sea surface temperatures and their relationships with tropospheric climate patterns. J Clim 12:2719–2733

Gan MA, Rao VB (1991) Surface cyclogenesis over South America. Mon Wea Rev 19:1293–1302

Giannini A, Saravanan R, Chang P (2004) The preconditioning role of Tropical Atlantic variability in the development of the ENSO teleconnection: implications for the prediction of Nordeste rainfall. Climate Dyn 22:839–855

Gordon C, Cooper C, Senior CA, Banks H, Gregory JM, Johns TC, Mitchell JFB, Wood RA (2000) The simulation of SST, sea ice extents and ocean heat transports in a version of the Hadley Centre coupled model without flux adjustments. Climate Dyn 16:147–168

Grimm AM (2003) The El Niño impact on the summer monsoon in Brazil: regional processes versus remote influences. J Clim 16:263–280

Grimm AM (2004) How do La Niña events disturb the summer monsoon system in Brazil? Climate Dyn 22:123–138

Grimm AM (2009) Variabilidade interanual do clima no Brasil. In: Cavalcanti IFA, Ferreira NJ, Justi da Silva MG, Silva Dias MAF (eds) Tempo e Clima no Brasil, chap 22, pp. 353–374. Editora Oficina de Textos, São Paulo

Grimm AM, Natori AA (2006) Climate change and interannual variability of precipitation in South America. Geophys Res Lett 33:L19706. doi:10.1029/2006GL026821

Grimm AM, Tedeschi RG (2009) ENSO and extreme rainfall events in South America. J Clim 22:1589–1609

Grimm AM, Zilli MT (2009) Interannual variability and seasonal evolution of summer monsoon rainfall in South America. J Clim 22:2257–2275

Grimm AM, Ferraz SET, Gomes J (1998) Precipitation anomalies in Southern Brazil associated with El Niño and La Niña events. J Clim 11:2863–2880

Grimm AM, Barros VR, Doyle ME (2000) Climate variability in Southern South America associated with El Niño and La Niña events. J Clim 13:35–58

Grimm AM, Vera CS, Mechoso CR (2005) The South American monsoon system. In: Chang C-P, Wang B, Lau N-CG (eds) The global monsoon system: research and forecast. WMO/TD 1266-TMRP 70, pp. 219–238. Available at http://www.wmo.int/pages/prog/arep/tmrp/documents/global_monsoon_system_IWM3.pdf

Grimm AM, Pal J, Giorgi F (2007) Connection between spring conditions and peak summer monsoon rainfall in South America: role of soil moisture, surface temperature, and topography in Eastern Brazil. J Clim 20:5929–5945

Janowiak JE, Xie P (2003) A global-scale examination of monsoon-related precipitation. J Clim 16:4121–4480

Jones C, Carvalho LMV (2002) Active and break phases in the South American monsoon system. J Clim 15:905–914

Jones RG, Murphy JM, Hassell DC, Woodage MJ (2005) A high resolution atmospheric GCM for the generation of regional climate scenarios. Hadley Centre Technical Note 63, Met Office, Exeter

Keller CF (2009) Global warming: a review of this mostly settled issue. Stoch Environ Res Risk Assess 23(5):643–676. doi:10.1007/s00477-008-0253-3

Kousky VE, Kagano MT, Cavalcanti IFA (1984) A review of the Southern Oscillation: oceanic-atmospheric circulation changes and related rainfall anomalies. Tellus 36A:490–504

Legates RD, Willmott CJ (1990) Mean seasonal and spatial variability in gauge-corrected global precipitation. Int J Climatol 10:111–127

Liebmann B, Allured D (2005) Daily precipitation grids for South America. Bull Am Meteorol Soc 86:1567–1570

Marengo J, Hastenrath S (1993) Case studies of extreme climatic events in the Amazon basin. J Clim 6:617–627

Marsland S, Haak H, Jungelaus J, Latif M, Röske F (2003) The Max-Planck-Institute global ocean/sea ice model with orthogonal curvilinear coordinates. Ocean Model 5:91–127

Nakicenovic N et al (2000) Special report on emissions scenarios. Cambridge University Press, Cambridge, 599 pp

Nogués-Paegle J, Mo K (2002) Linkages between summer rainfall variability over South America and sea surface temperature anomalies. J Clim 15:1389–1407

Nogués-Paegle J et al (2002) Progress in Pan American CLIVAR research: understanding the South American monsoon. Meteorologica 27:1–30

Pisciottano G, Diaz A, Cazes G, Mechoso CR (1994) El Niño-Southern Oscillation impact on rainfall in Uruguay. J Clim 7:1286–1302

Rao VB, Hada K (1990) Characteristics of rainfall over Brazil: annual variations and connections with the Southern Oscillation. Theor Appl Climatol 42:81–91

Roeckner E, Bäuml G, Bonaventura L, Brokopf R, Esch M, Giorgetta M, Hagemann S, Kirchner I, Kornblueh L, Manzini E, Rhodin A, Schlese U, Schulzweida U, Tompkins A (2003) The atmospheric general circulation model ECHAM5. Part I: model description, MPI Rep. 349. Max-Planck-Institute für Meteorologie, Hamburg, Germany

Ropelewski CF, Bell MA (2008) Shifts in the statistics of daily rainfall in South America conditional on ENSO phase. J Clim 21:849–865

Ropelewski CF, Halpert MS (1987) Global and regional scale precipitation patterns associated with the El Niño/Southern Oscillation. Mon Wea Rev 115:1606–1626

Ropelewski CF, Halpert MS (1989) Precipitation patterns associated with the high index phase of the Southern Oscillation. J Clim 2:268–284

Rowell DP (2005) A scenario of European climate change for the late twenty-first century: seasonal means and interannual variability. Climate Dyn 25:837–849

Rutland J, Fuenzalida H (1991) Synoptic aspects of the central Chile rainfall variability associated with the Southern Oscillation. Int J Climatol 11:63–76

Salio P, Nicolini M, Zipser EJ (2007) Mesoscale convective systems over southeastern South America and their relationship with the South American low-level jet. Mon Wea Rev 135:1290–1309

Satyamurti P, Ferreira CC, Gan MA (1990) Cyclonic vortices over South America. Tellus 42A:194–201

Severov DN, Mordecki E, Pshennikov VA (2004) SST anomaly variability in Southwestern Atlantic and El Niño/Southern Oscillation. Adv Space Res 33:343–347

Sinclair MR (1995) A climatology of cyclogenesis for the Southern Hemisphere. Mon Wea Rev 123:1601–1619

Stendel M, Schmidt T, Roeckner E, Cubasch U (2000) The climate of the 21st century: transient simulations with a coupled atmosphere-ocean general circulation model. Danmarks Klimacenter Report 00-6

Uvo CB, Repelli CA, Zebiak SE, Kushnir Y (1998) The relationships between tropical Pacific and Atlantic SST and Northeast Brazil monthly precipitation. J Clim 11:551–561

Velasco I, Fritsch JM (1987) Mesoscale convective complexes in the Americas. J Geophys Res 92(D8):9591–9613

Vera C, Higgins W et al (2006) Toward a unified view of the American monsoon system. J Clim 19:4977–5000

Wilks DS (1995) Statistical methods in the atmospheric sciences. Academic Press, New York

Zhou J, Lau WKM (2001) Principal modes of interannual and decadal variability of summer rainfall over South America. Int J Climatol 21:1623–1644